15th Triennial World Congress, Barcelona, Spain

MODELING AND CONTROL OF 3D EYE MOVEMENT WITH MUSCULOTENDON DYNAMICS

Ashoka D. Polpitiya * **Bijoy K. Ghosh** * **Clyde F. Martin** **
Lawrence Schovanec **

* *Department of Systems Science and Mathematics*
Washington University in St. Louis, USA
** *Department of Mathematics and Statistics*
Texas Tech University,USA

Abstract: Recent anatomical studies of extraocular muscles (EOM) demonstrate the stability of muscle paths. This is due to the fact that each rectus EOM passes through a pulley consisting of an encircling ring or sleeve of collagen. In this paper, the EOMs are modeled using the Hill type musculotendon complex and the effect of extraocular pulleys are studied. The model proposed by Martin and Schovanec in 1999, for horizontal eye movement has been used as a basic starting point. The extraocular pulleys are then introduced and analyzed mainly to study how Listing's law is enforced and how it implements an oculomotor plant which appears commutative to the brain.

Keywords: Listing's law, musculotendon dynamics, pulleys

1. INTRODUCTION

Modeling the eye plant in order to generate various eye movements, has been the topic among neurologists, physiologists, and engineers for a long time. The eyes rotate with three degrees of freedom, i.e., horizontal, vertical and torsional. Addressing the question of modeling the eye plant to mimic the realistic eye movements involves a three dimensional approach. Previous studies which used modeling as a means of understanding the control of three-dimensional eye movement have adopted two main approaches. One focusing on the details of the properties of the EOMs (Martin and Schovanec, 1998; Miller and Robinson, 1984) and the other focusing on control mechanisms for three-dimensional eye movement using over simplified linear models with all the details of the above EOM properties ignored (Raphan, 1998; Quaia and Optican, 1998).

About a decade ago Miller (Miller, 1989) noticed the stability of rectus EOM belly paths during eye movements. This provided strong evidence for EOM path constraint by pulleys. Each rectus EOM seemed to pass through a pulley consisting of an encircling ring or sleeve of collagen, located near the globe equator. Implications to ocular kinematics due to pulleys are discussed in this paper using the detailed ocular model first proposed by Martin and Schovanec (Martin and Schovanec, 1999) for horizontal saccadic eye movements.

If the eye is moved from one fixation to another, in theory, there are unlimited ways to orient the axis about which the eye rotates in 3-D space. But in reality, eye is constrained in its torsional freedom. This was first stated by Donders (1847), i.e., for steady fixation with the head upright, the actual positions of the eye are restricted in such a way that there is only one eye position for every gaze direction. This restricts the three-dimensional space of all possible orientations to a two-dimensional subspace. Listing and Helmholtz further investigated and determined to which two-dimensional subspace the eye is restricted. Listing's law, a specific case of more general Donders' law, states that any physiologic eye orientation can be reached from a particular eye position known as the primary position, by rotation around a single axis,

and that all such possible axes lie in a single plane known as Listing's plane. Unless the trajectory follows a radial line passing through the primary position, the rotation axis used to move the eye from one position to another, obeying Listing's law, tilts out of Listing's plane. Experiments done on normal human subjects and rhesus monkeys (Tweed and Villis, 1990; Haslwanter *et al.*, 1991) confirm this notion, i.e., if a trajectory is orthogonal to the radial line, the ocular rotation axis tilts out of Listing's plane by exactly half the angle of the eye's eccentricity for saccadic and smooth-pursuit eye movements. This is known as the "half-angle rule". Similar geometrical fact is observed for the vestibulo-ocular reflex (VOR) (Misslisch *et al.*, 1994). However the tilt angle here is only a quarter of the eye's eccentricity, hence "quarter-angle rule".

When pulleys were not known, Listing's law was presumed to be enforced by a neural circuitry issuing complex commands to the EOMs (Tweed *et al.*, 1992). But experiments have failed to identify such a neural substrate for Listing's law. It is also clear that the torsional component is generated somewhere downstream from the superior colliculus since the later encodes saccades as two dimensional (horizontal and vertical) rate of change of eye orientation. However, during VOR and sleep the Listing's law is violated implying that there is some kind of a neural basis.

The muscle path stability due to pulleys introduces a new mechanical basis on enforcing Listing's law. Figure 1 shows the arrangement of horizontal rectus EOMs. The rotational axis is always perpendicular to the plane containing the lines connecting pulleys with the scleral insertion. Therefore the rotational axis for straight ahead gaze in A, is vertical, i.e. perpendicular to the horizontal plane P_H. In B, the fixation is at a horizontally centered target at an elevation ϕ. The tilt of the rotational axis becomes $\phi/2$ and is perpendicular to the plane containing the lines connecting pulleys with the scleral insertion and the center to the scleral insertion. This 'half-angle plane' is shown as $P_{\phi/2}$. During VOR, the pulleys have to be displaced in such a way that the "quarter-angle rule" is satisfied. This implies the existence of a neural basis that causes the pulleys to shift posteriorly during VOR. One explanation to this phenomena is that there are separate motor neuron pools, or there is a way of adjusting the synaptic input weights in the same neuron pool, causing pulleys to move further posteriorly during VOR (Demer *et al.*, 2000).

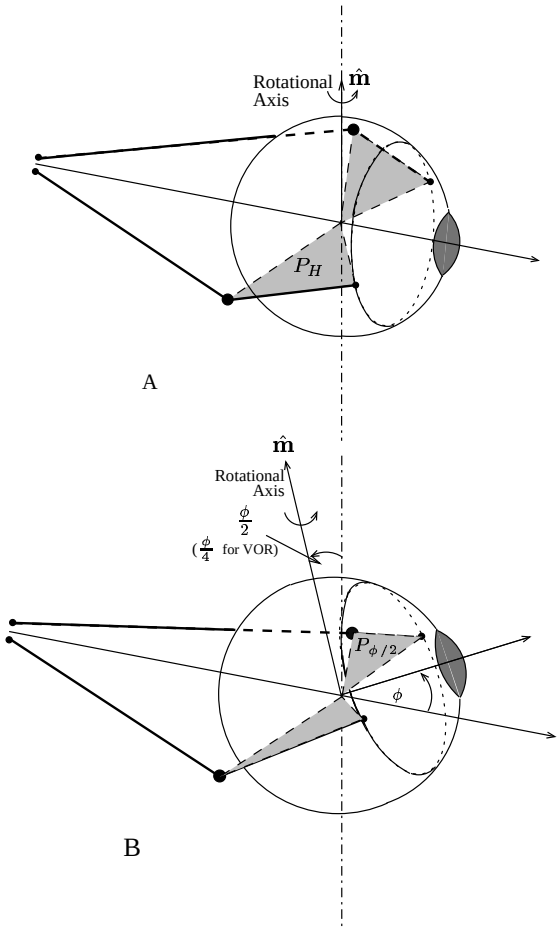

Fig. 1. Effect of pulleys on enforcing the Listing's law. Shown here are only the horizontal rectus EOMs. A: The rotational axis is vertical, i.e., perpendicular to the plane P_H. B: When the eye is in a secondary position of elevation of an angle θ, the rotational axis is perpendicular to the plane $P_{\phi/2}$(EOMs are shown in *thick lines* and pulleys as *dark dots*).

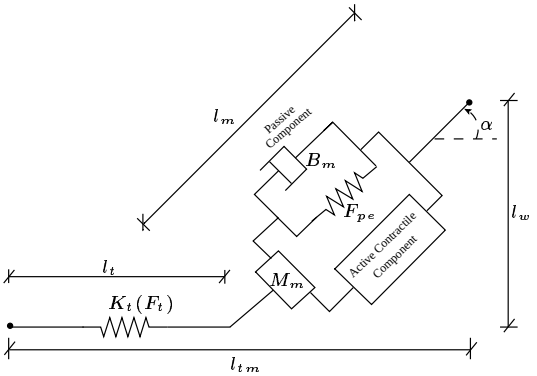

Fig. 2. Hill-type model of the musculotendon complex.

2. MODEL OF THE EYE

The model used here was first proposed by Martin and Schovanec (Martin and Schovanec, 1999; Martin and Schovanec, 1998) for horizontal saccadic eye movements. In the original model the geometrical implications due to pulleys were not considered. In this study, it is attempted to modify the model so that the resulting ocular plant would follow Listing's eye positions. The Hill-type model (Hill, 1938; Zajac, 1989) (Figure 2) used for the musculotendon complex, has been shown to incorporate enough complexity while remaining computationally practical.

The muscle of length l_m is in series and off-axis by a pennation angle α with the tendon of length l_t. The pennation effect in this model is an important feature which will be used later in this paper, to describe the pulley effect on EOMs. The total length of the musculotendon complex is l_{tm}. The muscle has two main components: an active force generator and a parallel passive component. The passive component consists of a parallel elastic element (F_{pe}) which describes the passive muscle elasticity and a damping component which corresponds to the passive muscle viscosity (B_m). The active component generates the active force for the muscle, which is the product of length-tension relation $f_l(l_m)$, velocity-tension relation $f_v(\dot{l}_m)$, and the activation level $a(t)$ (Zajac, 1989). In utilizing these relationships, analytical expressions that capture the qualitative properties of the curves will be used. Alternatively, a natural cubic spline can be fitted to the data when sufficient data is available.

In order to develop curves to describe the attributes of a generic muscle, appropriate scaling is done on the above parameters (Martin and Schovanec, 1999; Zajac, 1989). The scale parameters needed for each musculotendon include: maximal isometric active muscle force, F_o, optimal muscle length, l_o, pennation angle, α_o when $l_m = l_o$, and tendon slack length l_{ts}. All forces and lengths are scaled as $\tilde{F} = F/F_o$ and $\tilde{l}_m = l_m/l_o$.

The nonlinear passive muscle force which depends on the muscle length is commonly expressed as in Equation 1.

$$F_{pe}(l_m) = \begin{cases} (\frac{k_{ml}}{k_{me}})[exp(k_{me}(l_m - l_{ms})) - 1] & l_{ms} \le l_m < l_{mc} \\ k_{pm}(l_m - l_{mc}) + F_{mc} & l_m > l_{mc} \\ 0 & \text{otherwise} \end{cases} \quad (1)$$

Here the passive muscle slack length is l_{ms} corresponds to a length at which no force is generated. The transition length from the linear to nonlinear region is l_{mc} corresponding to the force F_{mc}.

The total active force generated is quantified as the product of the force-length and force-velocity curves and the resulting surface is scaled by muscle activation. Thus the active force is formulated as

$$F_{act} = F_o f_l(\tilde{l}_m) f_v(\tilde{v}_m) \times a(t)$$

where $\tilde{v}_m = \dot{\tilde{l}}_m$. Figure 3 shows the variation of muscle force with muscle length and velocity.

Muscle activation, $a(t)$, is related to the neural input $u(t)$ via the process known as contraction dynamics (Zajac, 1989). This process is known to be mediated through a calcium diffusion and is represented by a first order differential equation

$$\frac{da(t)}{dt} + \left[\frac{1}{\tau_{act}}(\beta + (1-\beta)u(t))\right] a(t) = \frac{1}{\tau_{act}} u(t)$$

where $0 < \beta < 1$ and τ_{act} is an activation time constant that varies with fast and slow muscle.

The tendon shown in Figure 2 as the series elastic element, assumed to behave non-linearly under minimal extension and then to become linear with stiffness constant k_s beyond a given length l_{tc} associated with a particular level of resisting force, F_{tc}. A common approach is to assume a model of the form

$$\dot{F}_t = K_t(F_t)\dot{l}_t \quad (2)$$

where

$$K_t(F_t) = \begin{cases} k_{te}F_t + K_{tl}, & 0 \le F_t < F_{tc} \\ k_s, & F_t \ge F_{tc} \end{cases}$$

Equation (2) can be integrated to obtain F_t:

$$F_t(l_t) = \begin{cases} \frac{k_{tl}}{k_{te}}(e^{k_{te}(l_t - l_{ts})} - 1), & l_{ts} \le l_t < l_{tc} \\ k_s(l_t - l_{tc}) + F_{tc}, & l_t > l_{tc} \\ 0, & otherwise \end{cases}$$

The total force in the muscle is the sum of the passive and active forces, $F_m = F_{pe} + F_{act} + B_m\dot{l}_m$. Muscle is also known to be isovolumic (Zajac, 1989). Hence the distance l_w remains constant. This gives

$$\dot{\alpha} = -\frac{\dot{l}_m}{l_m}\tan\alpha. \quad (3)$$

The equation of motion for the muscle mass is

$$M_m \frac{d^2(l_m \cos\alpha)}{dt^2} = F_t - (F_{act} + F_{pe} + B_m\dot{l}_m)\cos\alpha$$

i.e.,

$$M_m\ddot{l}_m = F_t\cos\alpha - \cos^2\alpha(F_{act} + F_{pe} + B_m\dot{l}_m) + \frac{M_m\dot{l}_m^2\tan^2\alpha}{l_m} \quad (4)$$

The eye is represented as a solid sphere with moment of inertia J_G. This sphere is rotating about a fixed point due to the moments of the six extraocular muscles attached to it. But the motion of the sphere is constrained by Listing's half angle rule (see Figure 1) and the muscles satisfying the isovolumic requirement (Zajac, 1989). The recent notion of enforcing the Listing's law due to pulley motion, can also be explained using this model. The constant volume requirement defines the pennation angle α (see Figure 4) as given in Equation (3). Listing's half-angle rule requires the rotational axis to be tilted backward by an angle of $\phi/2$ as shown in Figure 1. The moment vector $\hat{\mathbf{m}}$ which is along the rotational axis will be perpendicular to a plane given by $P_{\phi/2}$. Thus the radial distance vector from the center of the eye globe to the scleral insertion and the vector which represents the tendon force, lie on the plane $P_{\phi/2}$, i.e.,

$$(\boldsymbol{F_t} \times \boldsymbol{r}) \times \hat{\mathbf{m}} = 0$$

where $\boldsymbol{r}$ is the radial vector from the center of the eye to the scleral insertion. This uniquely determines the lateral and medial rectus pulley locations. The

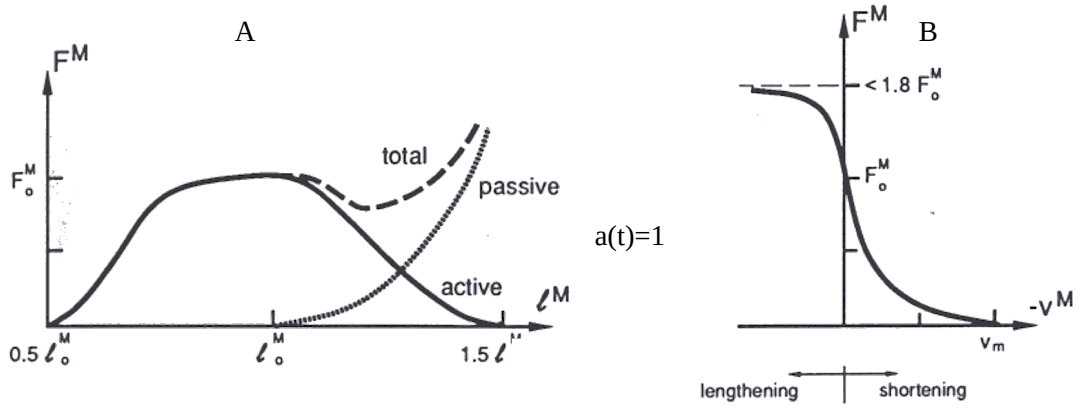

Fig. 3. **A**: Isometric Force-length relation and **B**: Force-velocity relation, for muscle with full activation, i.e., $a(t) = 1$ (Zajac, 1989)

kinematics of the superior and inferior rectus muscles (which are mainly responsible for vertical eye movement) follows a similar analysis.

The dynamics the eye, which is represented as a sphere rotating about a fixed point, are described by Euler's equations,

$$\begin{aligned} \sum M_x &= J_G \dot{\omega}_x, \\ \sum M_y &= J_G \dot{\omega}_y, \\ \sum M_z &= J_G \dot{\omega}_z \end{aligned} \tag{5}$$

This can be written in terms of the six moments generated by each muscle and a passive moment produced by orbital tissues, as,

$$\begin{bmatrix} \dot{\omega}_x \\ \dot{\omega}_y \\ \dot{\omega}_z \end{bmatrix} = \frac{1}{J_G} \left(\sum_{i=1}^{6} M_i + Mp \right) \tag{6}$$

$$= \frac{1}{J_G} \left(\sum_{i=1}^{6} \boldsymbol{F_t}_i \times \boldsymbol{r}_i + Mp \right) \tag{7}$$

In order to obtain the model in rotational velocities $\dot{\theta}$, $\dot{\phi}$, and $\dot{\psi}$, the notion of Eulerian angles (Goldstein, 1980) can be used. Thus taking $\boldsymbol{\omega} = (\omega_x \ \omega_y \ \omega_z)^T$ and $\bar{\theta} = [\theta \ \phi \ \psi]^T$,

$$\boldsymbol{\omega} = \underbrace{\begin{pmatrix} 0 & \cos\theta & \cos\phi \sin\theta \\ 0 & \sin\theta & \cos\phi \cos\theta \\ 1 & 0 & \sin\phi \end{pmatrix}}_{\mathbf{M}} \dot{\bar{\theta}}$$

i.e.,

$$\begin{aligned} \boldsymbol{\omega} &= \mathbf{M} \dot{\bar{\theta}} \\ \Rightarrow \dot{\boldsymbol{\omega}} &= \dot{\mathbf{M}} \dot{\bar{\theta}} + \mathbf{M} \ddot{\bar{\theta}} \end{aligned}$$

Let

$$\begin{aligned} \bar{\theta}_1 &= \bar{\theta} \\ \bar{\theta}_2 &= \dot{\bar{\theta}} \end{aligned}$$

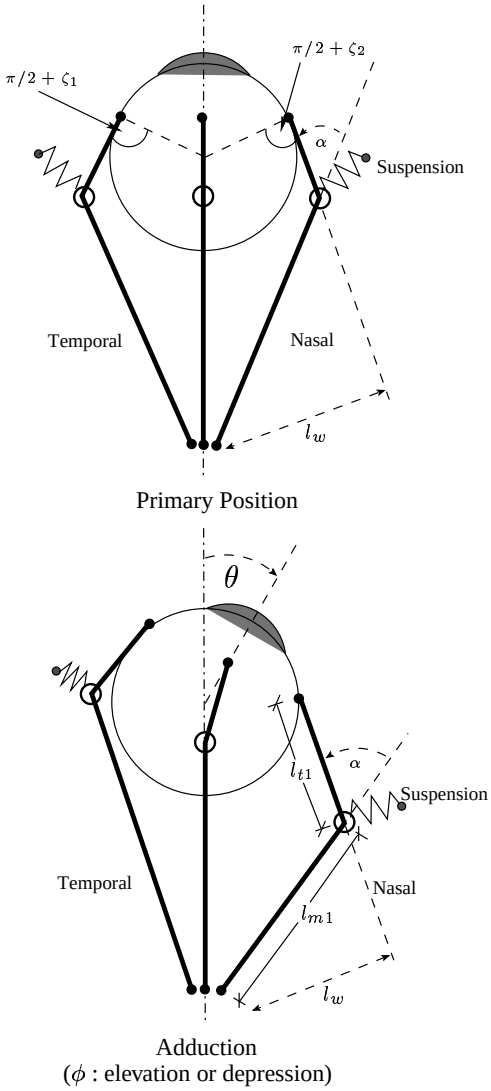

Fig. 4. Superior view of the eye showing the shifts in horizontal rectus pulley position required to satisfy half-angle rule in tertiary positions of adducted elevation and depression. Pulleys are shown as *rings*.

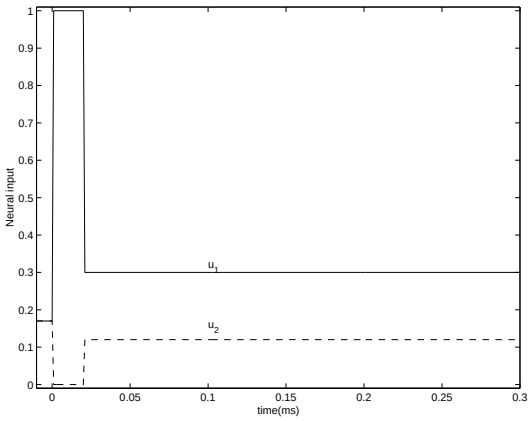

Fig. 5. Neural input to agonist (u_1) and antagonist (u_2) muscles

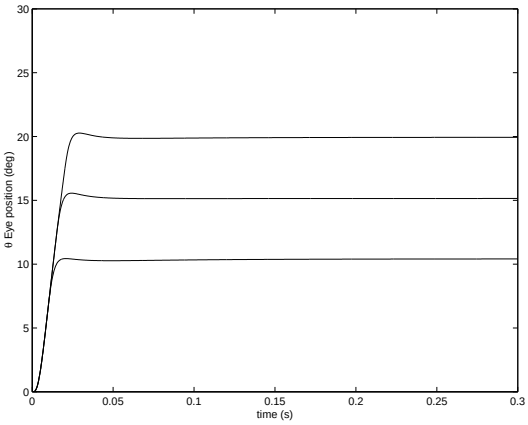

Fig. 6. Trajectories for 10^o, 15^o, 20^o saccades

then,

$$\begin{aligned}\dot{\bar{\theta}}_1 &= \bar{\theta}_2 \\ \dot{\bar{\theta}}_2 &= \ddot{\bar{\theta}} \\ &= \mathbf{M}^{-1}\left[\dot{\omega} - \dot{\mathbf{M}}\dot{\bar{\theta}}\right] \\ &= \mathbf{M}^{-1}\left[\frac{1}{J_G}\left(\sum_{i=1}^{6} \boldsymbol{F_t}_i \times \boldsymbol{r}_i + Mp\right) - \dot{\mathbf{M}}\bar{\theta}_2\right].\end{aligned}$$

The torsional component $\dot{\psi}$ can be eliminated using

$$\psi = \cos^{-1}\left(\frac{\sin(\theta)\sin(\phi)}{1+\cos(\theta)\cos(\phi)}\right),$$

(Miller and Robinson, 1984) which is due to Listing's law.

3. SIMULATIONS

Simulations were done only for few saccades for horizontal eye movements. Predetermined neural commands (Figure 5) were fed into the model and the resulting trajectories for eye position are plotted in Figure 6. The motorneurons' activity is composed of a tonic (Step) and a phasic (Pulse) component. During periods of fixation, only the Step is present, whereas during saccades both the Step and the Pulse are present (Fuchs *et al.*, 1988). The results are comparable to what is recorded experimentally (Robinson, 1964).

4. CONCLUSION

The model discussed in this paper, differs from the one proposed by (Martin and Schovanec, 1999) in the sense that it takes into account the mechanical implications due to recently discovered pulleys (Miller, 1989). Here, the notion of pulley motion enforcing Listing's law as opposed to the idea of the existence of a neural circuitry issuing complex commands to the EOMs, is proposed.

In order to satisfy the Listing's law, the rotational axis shown in Figure 1 should remain perpendicular to the plane containing the lines connecting pulleys with the scleral insertion and the center to the scleral insertion. For this to happen, the pulleys move in such a way that the muscle maintains a constant volume by keeping l_w (see Figure 4) constant throughout (Zajac, 1989).The purpose of the Listing's law is however still not very clear. One most suggesting idea is that it reduces the computational or physical work of some system (Tweed and Villis, 1990). For example, the work of the perceptual system may be simplified by choosing one orientation for a given gaze direction (fixing the "torsional" component according to Donders' law).

Further work can be done on improving the model that has been discussed here. Current work on the model with three pairs of muscles, tries to study the characteristics of motoneuron activities which produce saccadic eye movements in accordance with the Listing's half-angle rule. It would also be necessary to look at the inverse control problem so that for a specific trajectory, the exact values of the innervations to the three pairs of muscles can be determined.

5. REFERENCES

Demer, J.L., S. Oh and V. Poukens (2000). Evidence for active control of rectus extraocular muscle pulleys. *Invest Opthalmol Vis Sci.* **41**, 1280–1290.

Fuchs, A.F., C.A. Scudder and C.R.S. Kaneko (1988). Discharge patterns and recruitment order of identified motoneurons and interneuclear neurons in the monkey abducens nucleus. *J. of Neurophysiology* **60**, 1874–1895.

Goldstein, H. (1980). *Classical Mechanics*. Addison-Wesley. MA.

Haslwanter, T., D. Straumann, K. Hepp, B.J.M. Hess and V. Henn (1991). Smooth pursuit eye movements obey listing's law in the monkey. *Exp.Brain Res.* **87**, 470–472.

Hill, A.V. (1938). The heat of shortening and dynamic constants of muscle. *Proc. Roy. Soc. B.* **126**, 136–195.

Martin, C.F. and L. Schovanec (1998). Muscle mechanics and dynamics of ocular motion. *J. of Mathematical Systems, Estimation and Control* **8**, 1–15.

Martin, C.F. and L. Schovanec (1999). The control and mechanics of human movement systems. *Progress in Systems and Control Theory* **25**, 173–202.

Miller, J.M. (1989). Functional anatomy of normal human rectus muscle. *Vision Res.* **29**, 223–240.

Miller, J.M. and D.A. Robinson (1984). A model of the mechanics of binocular alignment. *Computers and Biomedical Research* **17**, 436–470.

Misslisch, H., D. Tweed, M. Fetter, D. Sievering and E. Koenig (1994). Rotational kinematics of the human vestibuloocular reflex. iii. listing's law. *J. of Neurophysiology* **72**, 2490–2502.

Quaia, C. and L.M. Optican (1998). Commutative saccadic generator is sufficient to control a 3-d ocular plant with pulleys. *J. of Neurophysiology* **79**, 3197–3215.

Raphan, T. (1998). Modeling control of eye orientation in three dimensions. 1. role of muscle pulleys in determining saccadic trajectory. *J. of Neurophysiology* **79**, 2653–2667.

Robinson, D.A. (1964). The mechanics of human saccadic eye movement. *J. of Physiology* **174**, 245–264.

Tweed, D. and T. Villis (1990). Geometric relations of eye position and velocity vectors during saccades. *Vision Res.* **30**, 111–127.

Tweed, D., M. Fetter, S. Andreadaki, E. Koenig and J. Dichgans (1992). Three-dimensional properties of human pursuit eye movements. *Vision Res.* **32**, 1225–1238.

Zajac, F.E. (1989). Muscle and tendon: Properties, models, scaling, and application to biomechanics and motor control. *CRC Critical Reviews in Biomedical Engineering* **17**, 359–411.